TRENDS IN SCIENCES 2026; 23(9): 12064
https://doi.org/10.48048/tis.2026.12064 RESEARCH ARTICLE

MgFe-LDH and MgFe-LDH-Derived Mixed Oxides as Effective Amoxicillin Adsorbents: A Comparison Study

Swasmi Purwajanti[1], Jasmine Cupid Amaratirta[2], Razita Izzati[3], Nur Rohmah[1] Akmal Zulfi[4], Yulianto Agung Rezeki[2,*] and Aep Patah[3]

[1]Research Center for Electronics, National Research and Innovation Agency (BRIN), Bandung 40135, Indonesia
[2]Department of Physics Education, Faculty of Teacher Training and Education, University of Sebelas Maret, Surakarta 57126, Indonesia
[3]Division of Inorganic and Physical Chemistry, Faculty of Mathematics and Natural Sciences, Institut Teknologi Bandung, Bandung 40132, Indonesia
[4]Research Center for Environmental Technology and Clean Technology, National Research and Innovation Agency (BRIN), Banten 15314, Indonesia

([*]Corresponding author's e-mail: yarezeki@staff.uns.ac.id)

Received: 26 September 2025, Revised: 20 January 2026, Accepted: 9 February 2026, Published: 1 April 2026

Abstract

Antibiotic contamination, particularly from amoxicillin, poses serious ecological and health risks due to its persistence in aquatic systems. This study hypothesized that MgFe-layered double hydroxide (MgFe-LDH) synthesized from salt-industry by-product (bittern) and its calcined derivative (MgFe-CLDH) can act as sustainable and efficient adsorbents for amoxicillin removal. MgFe-LDH was prepared via co-precipitation and partially calcined at 450 °C to form MgFe-CLDH. Both materials were characterized by XRD, SEM, FTIR, and BET analyses, and their adsorption behaviors were evaluated under varying pH, contact time, initial concentration, and co-existing ions. MgFe-LDH and MgFe-CLDH exhibited maximum adsorption capacities of 82.79 and 86.94 mg/g, respectively. Kinetic studies showed that MgFe-LDH followed a pseudo-second-order model (chemisorption), whereas MgFe-CLDH followed a pseudo-first-order model (physisorption). Freundlich isotherm fitting indicated multilayer adsorption on heterogeneous surfaces. Regeneration tests confirmed stable reusability, with optimal performance observed after the second adsorption cycle. These findings validate the hypothesis and demonstrate that MgFe-based LDH adsorbents derived from industrial by-products offer a cost-effective route for antibiotic wastewater remediation.

Keywords: Amoxicillin, Layered doubled hydroxides, Adsorption, Bittern, Co-precipitation

Introduction

Antibiotics are widely used across various sectors, including healthcare, pharmaceuticals, veterinary medicine, and agriculture [1]. As antimicrobial agents, they are essential for combating bacterial infections and have become indispensable in modern medical treatment [2]. The occurrence of antibiotics as emerging contaminants in aquatic environments has been increasingly recognized as a significant ecological threat, necessitating urgent intervention by governmental bodies and environmental regulatory agencies worldwide [1-3]. Due to incomplete metabolism in humans and animals, around 30% of the ~90% of administered antibiotics are excreted unchanged and discharged into wastewater streams [4]. As a result, amoxicillin has been detected at high concentrations in various water bodies, for example, up to 1,172,000 ng/L in hospital effluents, 66 - 5,230 ng/L in municipal wastewater, and as high as 460 µg/L in coastal discharge zones [5,6]. Meta-analyses also consistently report its presence in surface waters at ng/L to tens-of-ng/L levels [7]. Moreover, self-medication

practices further contribute to the uncontrolled release of antibiotics into the environment, intensifying concerns related to antibiotic pollution.

One of the most commonly used antibiotics is amoxicillin (AMX), a broad-spectrum β-lactam antibiotic frequently prescribed for infections such as respiratory tract infections, urinary tract infections, and skin infections [3,8]. Studies have shown that over 80% of orally administered AMX is excreted unchanged in urine within 2 h of intake [3,9]. The presence of AMX has recently been detected in various aquatic environments, including surface water, municipal and industrial wastewater, and hospital effluents with concentrations ranging from nanograms per liter (ng/L) to milligrams per liter (mg/L) [10-12]. A study by Owusu-Ofori *et al.* [13] found that amoxicillin is the most commonly used antibiotic in self-medication practices, accounting for 72.4% of reported cases. This widespread use substantially contributes to the persistence of pharmaceutical pollutants, particularly amoxicillin, in the environment.

The presence of antibiotics in the aquatic environment poses serious ecological threats. One of the most critical consequences is the development of antibiotic resistance [13]. Continuous exposure of microbial communities to low concentrations of antibiotics promotes the emergence of resistant bacterial strains. This not only reduces the effectiveness of current treatments but also facilitates the evolution of new, more dangerous infections. According to Murray *et al.* [15], antimicrobial resistance directly caused an estimated 1.27 million deaths globally in 2019, making it one of the most pressing public health challenges.

To mitigate the environmental impact of antibiotic contamination, several remediation methods have been explored, including nanofiltration membranes, coagulation/flocculation, advanced oxidation processes (AOPs), and adsorption [9,10,14,15]. Among these, adsorption has emerged as a promising approach due to its simplicity, cost-effectiveness, operational flexibility, and reusability. Pourhakkak *et al.* [11] emphasized that an ideal adsorbent should possess high selectivity, large adsorption capacity, low cost, and regenerability. However, developing economically and environmentally friendly adsorbents with higher adsorption capacities for spharmaceutical ingredients is still needed. One class of materials that has gained increasing attention for environmental remediation is Layered Double Hydroxides (LDHs). LDHs are 2-dimensional nanomaterials with positively charged metal hydroxide layers and interlayer anions, similar in structure to clays [12]. They exhibit high anion exchange capabilities, excellent thermal stability, large specific surface area, their multifarious composition, low cost, tunable morphological features, required porosity anfacile synthesis techniques—properties that make them particularly suitable as adsorbents [16,17]. Furthermore, LDHs has shown adsorption properties towards many organic contaminants through electrostatic binding unto the positively charged surface. The general formula of LDHs is $[M^{2+}_{1-x}M^{3+}_{x}(OH)_2]^{x} + [A^{n-}]_{x/n} \cdot mH_2O$, where $M^{2+}$and M^{3+} represent divalent and trivalent metal cations, respectively [18]. The calcined form of LDHs, called calcined LDHs also shows a potency for antibiotic adsorption owing to the better reconstruction ability as reported by Park *et al.* [19].

Among the various LDH systems, MgFe-LDH a combination of magnesium (Mg^{2+}) and iron (Fe^{3+})—shows great potential as an antibiotic adsorbent. When subjected to calcination at elevated temperatures, MgFe-LDH transforms into MgFe-CLDH, a mixed metal oxide that retains a unique "memory effect." This effect enables MgFe-CLDH to reconstruct its original LDH structure upon rehydration in aqueous environments, thereby enhancing its adsorption capacity and structural adaptability [20]. To reduce costs and promote sustainability, the use of industrial by-products as raw materials for LDH synthesis is also being explored. Indonesia, with over 95,000 km of coastline, has a significant marine resource potential, including widespread salt production [21]. One by-product of salt production is bittern; a concentrated liquid residue rich in inorganic ions, particularly magnesium. Bittern has been reported to contain approximately 31,740 ppm of magnesium, making it a valuable and cost-effective source of Mg^{2+} for LDH synthesis [22].

In this study, for the first time we compare the MgFe-LDH and metal-oxide derived MgFe-LDH as adsorbent of AMX from aqueous solutions and study the adsorption performance also plausible mechanism of both classes of adsorbent. MgFe-LDH was synthesized

via co-precipitation at pH 12, utilizing bittern as the magnesium precursor. Part of the synthesized material was calcined at 450 °C to produce MgFe-CLDH. Both MgFe-LDH and MgFe-CLDH were then applied as adsorbents for the removal of amoxicillin from aqueous solutions. The adsorption process was analyzed by evaluating the effects of pH, contact time, and initial concentration of amoxicillin. The remaining concentration of amoxicillin in solution was determined using UV-Vis spectrophotometry at its maximum absorption wavelength of 230 nm. To further assess the adsorbents' practical performance, regeneration tests were conducted to evaluate their reusability, and co-existing ion tests were performed to examine the impact of common aqueous ions on adsorption efficiency. This was based on the fact that natural waters contain various ions such as Na^+, K^+, Ca^{2+}, Mg^{2+}, Cl^-, $SO_4{}^{2-}$, $NO_3{}^-$, and $HCO_3{}^-$, which may influence the adsorption process [23]. Understanding these interferences is crucial for evaluating the feasibility of using MgFe-based adsorbents under realistic environmental conditions. Moreover, the successful synthesis of LDH and mixed oxide from bittern paves the way for their practical application in real-world environmental remediation.

Materials and methods

Materials

Bittern used was from saltpond in Madura derived from salt industry waste and has been filtered. Additionally, $FeCl_3 \cdot 6H_2O$, NaOH, and NH_2CO_3 are were supplied form Sigma-Aldrich. The solvent used for some materials was MilliQ water with conductivity of 16 ohm. In the adsoprtion testing process, amoxicillin was used along with several salts and acids, named NaCl, $MgCl_2$, KCl, HCl, H_3PO_4, and H_2SO_4. AMX was supplied from Sigma-Aldrich and used without further purification.

MgFe-LDH and MgFe-CLDH synthesis

The synthesis scheme of MgFe-LDH and MgFe-CLDH is illustrated in **Figure 1**. The synthesis was conducted using the coprecipitation method, starting with the preparation of filtered bittern. Then, $FeCl_3 \cdot 6H_2O$ and bittern mixed with a molar of Mg^{2+}: Fe^{3+} of 3:1. This mixture was then slowly dripped into a Duran bottle along with a solution consisting of Na_2CO_3 (0.4 mol/L) and NaOH (1.5 mol/L) in a volume of 100 mL, with the rate of addition of both solutions being the same. The pH of the solution was adjusted to reach pH 12 using NaOH as a strong base.

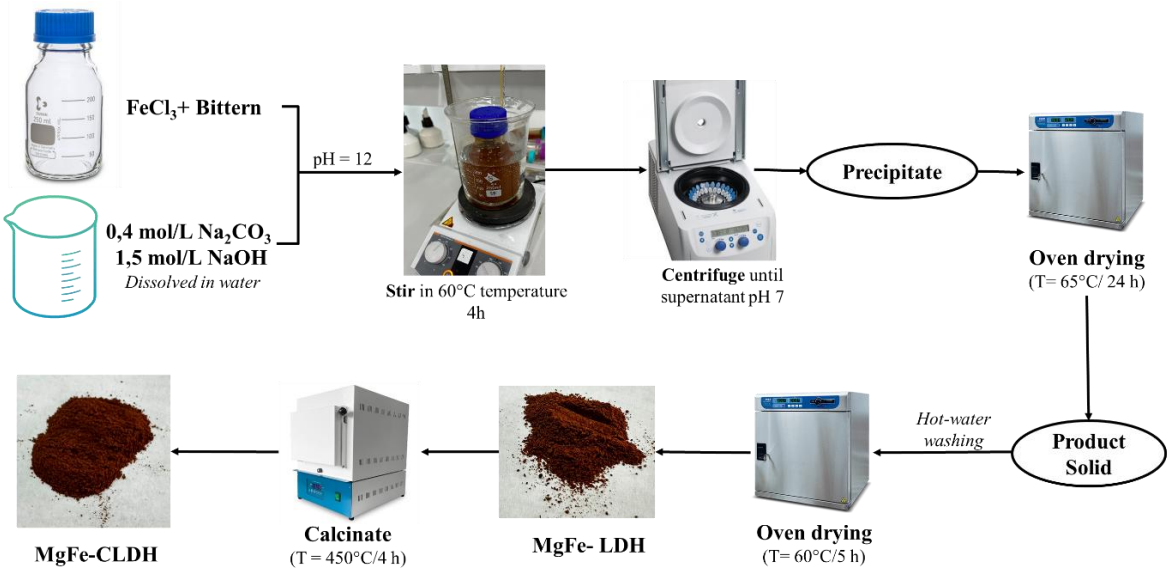

Figure 1 Synthesis scheme of MgFe-LDH and MgFe-CLDH.

Subsequently, the solution was heated at 60 °C with constant stirring for 4 h. The result of heating was centrifuged at 2,000 rpm for 10 min repeatedly until the pH of the supernatant reached 7. The precipitate obtained was then dried in an oven at 65 °C for 24 h, washed with hot water, and re-dried at 60 °C for 5 h. To produce MgFe derived mixed oxide, denoted as MgFe-

CLDH, the synthesized MgFe-LDH was calcined in a furnace at 450 °C.

Amoxcillin solution preparation

Amoxicillin solution was prepared by dissolving 1 g of amoxicillin into 1 L of distilled water so as to form amoxicillin stock solution with a concentration of 1,000 ppm. The solution was then diluted to the required concentration range as a standard solution to create a calibration curve.

Characterization of MgFe-LDH and MgFe-CLDH

Samples of MgFe-LDH and MgFe-CLDH, both before and after adsorption, were prepared at a mass 0.5 g for comprehensive physicochemical analysis. The crystalline structures were examined using X-ray diffraction (XRD) performed on a Rigaku Miniflex instrument with Cu $K\alpha$ radiation ($\lambda = 0.1540$ nm). The measurements were made in the 2θ angle range of 5° to 70° with an interval of 0.01°, allowing for detailed identification of crystal phases and structural changes due to calcination and adsorption processes. The surface morphology and microstructural features of the samples were analyzed via Scanning Electron Microscope (SEM) using a JEOL JSM-IT300 InTouchScope with a voltage of 20.0 kV. Chemical functional groups and bonding interactions were analysed using Fourier-transform infrared (FTIR) spectroscopy with KBr pellet samples, covering the wavenumber range of 4,000 to 400 cm^{-1}. Finally, the specific surface areas of the synthesized MgFe-LDH and MgFe-CLDH were analyzed using BET surface area method with N_2 adsorption/desorption. BET analysis was performed using Quantachrome NovaWin.

Adsorption test

Adsorption tests were conducted to evaluated the adsorption performance of MgFe-LDH and MgFe-CLDH under various operating parameters, including solution pH, contact time, and initial amoxicillin concentration. Additional tests were performed to examine adsorbent regeneration potential and the influence of co-existing ions commonly found in wastewater.

Effect of pH

To determine the optimal pH for adsorption, 10 mg of adsorbent was added to 10 mL of 50 ppm amoxicillin solution was adjusted to pH 2, 4, 6, 8, and 10 using HCl or NaOH. The mixtures were sieved at room temperature (25 °C) with an orbital shaker at 200 rpm for 180 min. After filtration, the residual concentration was analyzed as before.

Effect of contact time

Adsorption kinetics were analyzed by varying the contact time. A total of 10 mg of adsorbent was mixed with 10 mL of 150 ppm amoxicillin solution (at the optimal pH). The mixtures were shaken at 200 rpm at room temperature for different durations, namely 5, 10, 20, 40, 60, 90, 120, and 180 min. After filtration, the residual concentration was analyzed as before.

Effect of initial concentration

To construct adsorption isotherms, 10 mg of adsorbent was added to 10 mL of amoxicillin solutions with varying initial concentrations of 10, 20, 50, 80, 100, 150, 200, and 250 ppm (with optimum pH and fixed contact time for 120 min) were also sieved under similar conditions. After the stirring process was complete, the solution was filtered using filter paper and the absorbance was measured with a UV-Vis spectrophotometer at a wavelength of 230 nm and the residual concentration of NOR was determined by substituting into the standard curve, and the equilibrium adsorption capacity was calculated. The adsorption capacity can be calculated by Eq. (*1*).

$$Q_e = \frac{V(C_0 - C_e)}{m} \quad (1)$$

where $Q_e(mg \cdot g^{-1})$ is the equilibrium adsorption capacity, respectively; C_0 $(mg.L^{-1})$ and $C_e(mg.L^{-1})$ are the initial and equilibrium concentrations of the target pollutant. All tests were performed in duplo and the presented value in this paper is the average result.

MgFe-LDH regeneration test

The regeneration ability of MgFe-LDH was evaluated by regeneration method. The regeneration method used was thermal regeneration. MgFe-LDH that had been used in the first adsorption was calcined at 450

°C for 4 h and then reused for the adsorption process. Adsorption was carried out 4 times using the same conditions and analyzed for amoxicillin adsorption capacity through absorbance measurements using a UV-Vis spectrophotometer at a wavelength of 230 nm. All test variations were duplo.

Co-existing ion test

The effect of co-existing ions in water was investigated to identify the types of ions, namely Na^+, K^+, Mg^{2+}, SO_4^{2-}, Cl^-, and $H^2PO_4^-$, that might be present in wastewater and to understand the competition between adsorbates and these ions. A volume of 10 mL of ion solutions with varying concentrations of 0.01, 0.05 and 0.1 M was mixed with 100 ppm amoxicillin solution, then 10 mg of adsorbent was added. The mixture was sieved at room temperature for 120 min, and each test was performed Duplo to validate the results.

After they were shaken, the solutions were centrifuged and the content of AMX in the solution was determined using UV/Visible-Agilent Spectrophotometer and calculated based on the linear correlation between absorbance of AMX at 230 nm and AMX concentration. The calibration curve of AMX was presented in **Figure S1**.

Results and discussion

Characterization of MgFe-LDH and MgFe-CLDH

The structural, morphological, and surface properties of MgFe-LDH and MgFe-CLDH were characterized using X-ray diffraction (XRD), scanning electron microscopy (SEM), Fourier-transform infrared spectroscopy (FTIR), and Brunauer-Emmett-Teller (BET) surface area analysis to reveal the effect of calcination on the adsorbent materials.

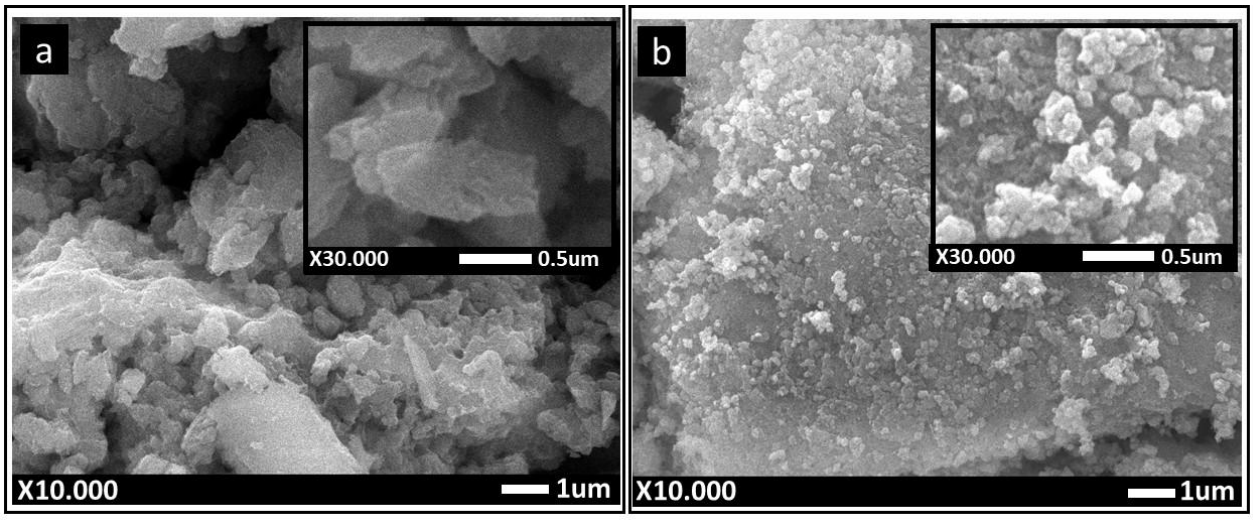

Figure 2 The SEM morphology of as-prepared MgFe-LDH (a) and MgFe-CLDH (b).

Figure 2(a) show the morphology of as-prepared MgFe-LDH, exhibiting disc-like structures characteristic of LDH. The small particles observed on these discs are likely minor impurities [24]. **Figure 2(b)** demonstrates that the morphology of as-prepared MgFe-CLDH is irregular compared to that of MgFe-LDH. This is attributed to the formation of metal oxides as well as deintercalation and decomposition in the space between LDH layers. After calcination, the sample became more amorphous and exhibited a flower-like surface, consistent with the findings of Golban *et al.* [25].

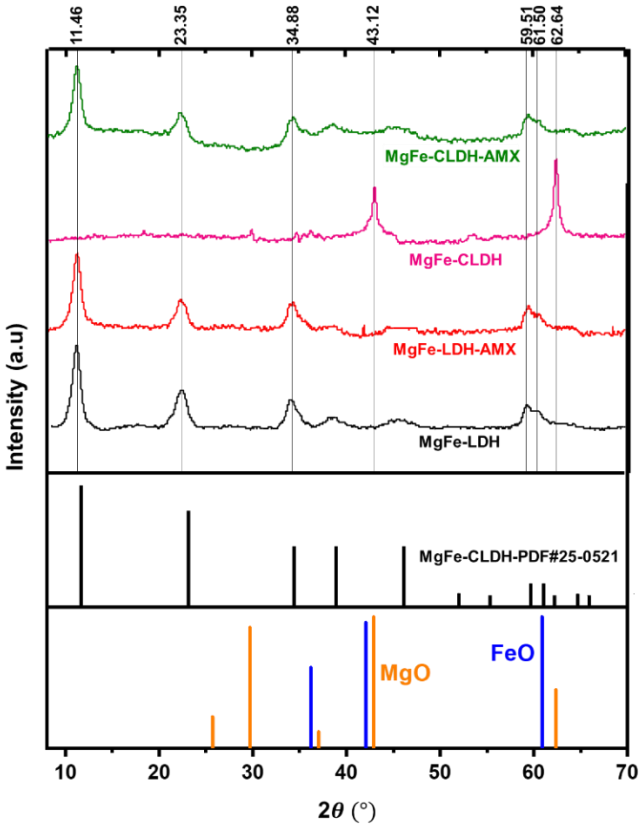

Figure 3 MgFe-LDH and MgFe-CLDH diffractograms.

These morphological observations are supported by **Figure 3**, which presents the X-ray diffraction patterns of MgFe-LDH and MgFe-CLDH samples before adsorption. MgFe-LDH shows peaks at 2θ of 11.46,23.35,34.88,59.51, and 61.50, corresponding to the (003), (006), (009), (110), and (113) [26]. This indicates a well-ordered layered structure and uniform metal dispersion of metal ions within the hydroxide layers [27]. These reflections are consistent with the reference hydrotalcite phase MgFe-LDH (JCPDS 25-0521), as also shown by Li *et al.* [30], who used this card to verify the successful formation of MgFe-LDH prior to thermal treatment. After calcination, MgFe-CLDH reveals the disappearance of characteristic MgFe-LDH peaks, accompanied by the appearance of 2 broad at 43.12° and 62.64°. These peaks match to the (200) and (220) planes reflections of periclase MgO (JCPDS 45-0496), reported similar MgO reflections at ~42.9° and 62.3° following thermal decomposition of MgFe-LDH nanosheets [28]. The position and broadening of these peaks also fall between those of pure MgO and FeO, suggesting the possible formation of a MgO-FeO solid solution, which Li *et al.* [30] observed when Fe species partially dissolved into the MgO lattice during thermal treatment at ≥ 400 °C. This interpretation is also consistent with observations by Fletcher *et al.* [31], who demonstrated that MgO-based mixed metal oxides often show overlapping MgO and Fe oxide-related reflections rather than distinct spinel peaks when the material is poorly crystalline or only partially transformed [29]. This transition reflects deintercalation and structural collapse of the LDH, consistent with the amorphous morphology observed in SEM [30].

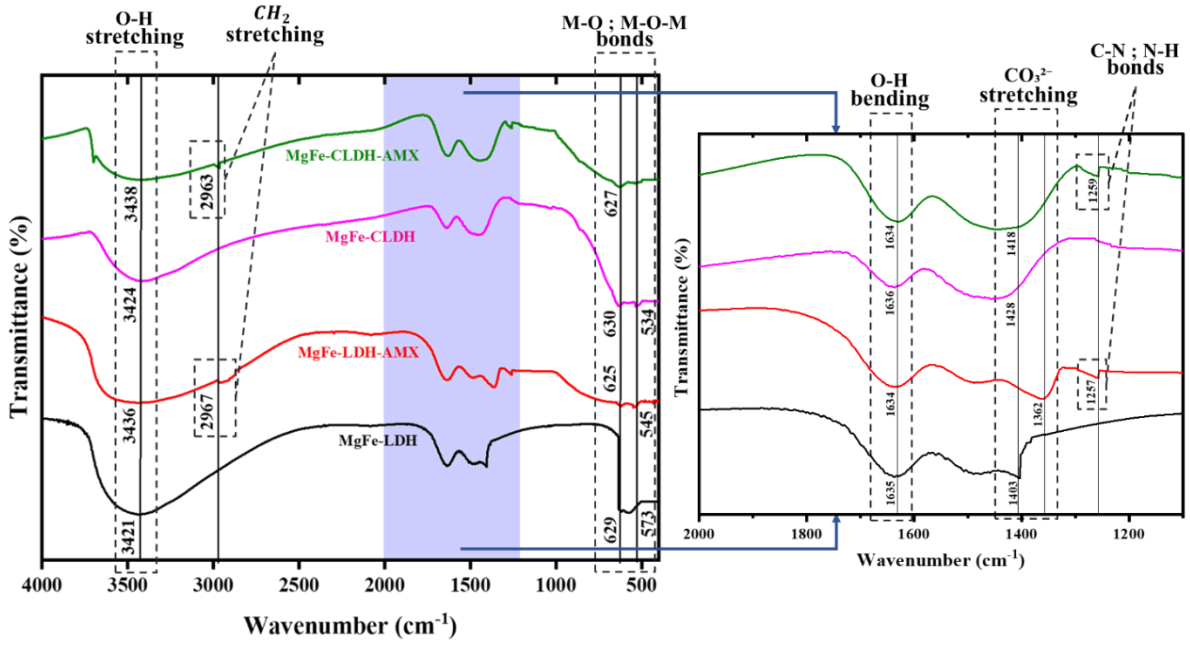

Figure 4 FTIR spectra of MgFe-LDH and MgFe-CLDH.

The Fourier Transform Infrared (FTIR) spectra confirm these structural changes as shown in **Figure 4**. MgFe-LDH exhibits characteristic O–H stretching (~3,400 cm^{-1}), H–O–H bending (~1,630 cm^{-1}), and strong CO_3^{2-} bands (~1,360 -1,430 cm^{-1}), typical of interlayer anions in LDHs. In contrast, these bands are significantly reduced or absent in MgFe-CLDH, reflecting the elimination of water molecules and interlayer carbonates, consistent with the deintercalation process seen in XRD [26,27]. The peaks observed below 800 cm^{-1} indicated the vibrational of metal oxides M–O and M–O–M bonds (M = Mg/Fe) [27,31].

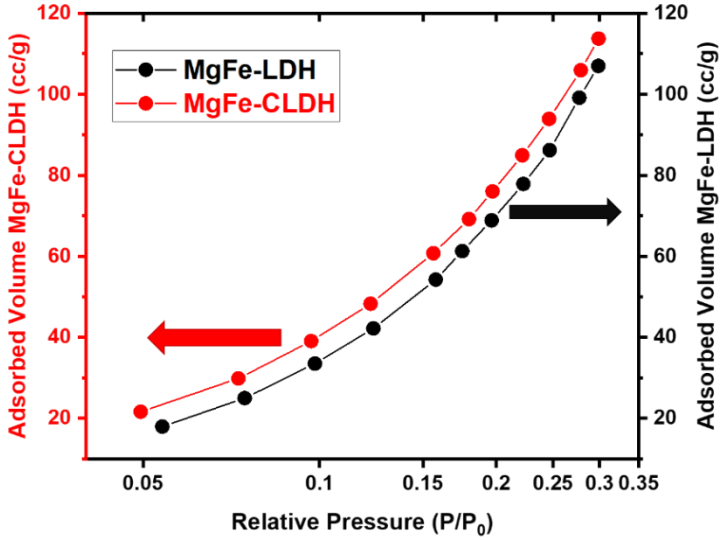

Figure 5 N_2 adsorption curves on MgFe-LDH and MgFe-CLDH.

Furthermore, Bruner-Emmet-Teller (BET) analysis reveals that both MgFe-LDH and MgFe-CLDH exhibit as shown in **Figure 5**. The N_2 adsorption curve on MgFe-LDH and MgFe-CLDH exhibits a type III isotherm. The increase in adsorption with increasing relative pressure and value of c less than 1 ($c < 1$) indicates the formation of multilayers and demonstrates that adsorbate-adsorbate interactions are more dominant than adsorbent–adsorbate interactions. The surface area of MgFe-LDH reaches 693.157 m^2/g, while that of

MgFe-CLDH is 590.307 m²/g, indicating a reduction due to calcination. This decrease is attributed to structural densification and partial pore blockage, consistent with the collapse of the layered structure observed in SEM and the disappearance of characteristic LDH peaks in XRD [32]. Despite this decrease, the relatively high surface area of MgFe-CLDH suggests that the Fe arrangement within the LDH matrix was not completely restored, as also evidenced by the flake-like morphology observed in SEM images (**Figure 2(b)**).

The effect of pH on adsorption performance

The effect of pH on the adsorption performance was investigated by varying the pH of the across a range of 2, 4, 6, 8, and 10. The experimental results indicate that the highest adsorption capacity for MgFe-LDH was observed at pH 6, with a value of 10.52 mg/g, while MgFe-CLDH exhibited its maximum adsorption capacity at pH 4, reaching 46.65 mg/g. Depsite these peaks, the overall variation in adsorption capacity across the tested ph range (2 until 10) was not significantly different, as showed in **Table 1**.

Table 1 Adsorption capacity at varying pH.

pH	q_e MgFe-LDH (mg/g)	q_e MgFe-CLDH (mg/g)
2	7.61	45.79
4	10.29	46.65
6	10.52	44.59
8	9.17	44.64
10	10.38	42.05

The less difference in adsorption capacity from pH 2 to 8 indicates that MgFe-LDH and MgFe-CLDH can adsorb amoxicillin over a wide range of pH conditions. Therefore, the adsorption performance of both materials over a wide pH range (from highly acidic to mildly alkaline) indicates their potential use in the treatment of environments or wastewater with significant pH variations. These results indicate that adsorption of amoxicillin onto MgFe-based adsorbents is governed by chemisorption-dominated mechanisms, which accounts for the relatively weak dependence on solution pH. Furthermore, pH 6 was selected for further adsorption studies on MgFe-LDH and considered as optimal compromise between AMX speciation, LDH structural integrity and anion exchange efficiency, and pH 4 for MgFe-CLDH, based on their respective optimal performance.

The pH-dependent adsorption behavior of amoxicillin can be explained by the combined effects of surface charge characteristics of MgFe-LDH-based adsorbents and the speciation of amoxicillin in aqueous solution. Amoxicillin exists predominantly in a protonated form at pH < 2.7, leading to electrostatic repulsion with the positively charged LDH surface and reduced adsorption efficiency. In the pH range of 2.7 - 7.4, amoxicillin is present mainly in a zwitterionic or neutral form, minimizing electrostatic repulsion and enabling favorable hydrogen bonding and surface complexation, which promotes rapid adsorption kinetics and higher uptake [33,34]. At pH values above 7.4, amoxicillin becomes negatively charged, resulting in strong electrostatic attraction toward the positively charged LDH surface; however, increased competition with hydroxyl ions and surface site saturation can limit further adsorption enhancement [35,36]. These pH-dependent electrostatic interactions directly influence adsorption kinetics, indicating that the adsorption process is primarily governed by surface-controlled mechanisms rather than diffusion-limited intercalation. Similar relationships between molecular speciation, surface chemistry, and adsorption kinetics have been widely reported for antibiotic adsorption on LDH-based materials. In addition to that, at low pH there is a tendency for MgFe-LDH partial dissolution which may reduce effective adsorption sites and alter layer structure. Meanwhile mixed metal oxides are generally more chemically stable but lack interlayer anion exchange capacity.

The plausible mechanism of pH-dependent AMX adsorptuin onto MgFe-LDH and MgFe-CLDH is illustrated in **Figure 6**. As schematically illustrated in **Figure 6**, adsorption of amoxicillin on MgFe-LDH and

MgFe-CLDH is governed by a combination of electrostatic interactions, surface complexation, hydrogen bonding, and interlayer anion exchange. The coexistence of these mechanisms explains both the observed pH-dependent optima and the relatively stable adsorption performance across a wide pH range.

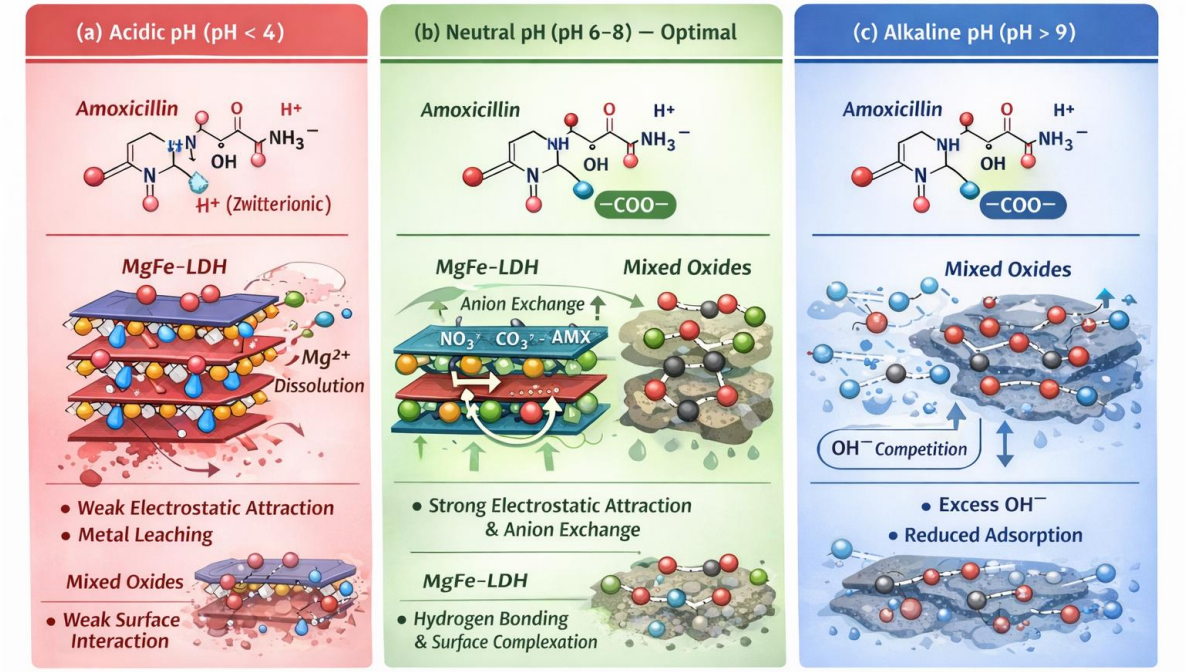

Figure 6 pH-dependent adsorption mechanism of AMX on MgFe-LDH and MgFe-CLDH: (a) weak electrostatic interactions and partial dissolution dominate under acidic conditions (pH < 4); (b) strong electrostatic attraction and anion exchange enable optimal adsorption at neutral pH (pH 6 - 8); (c) excess OH^- competition results in reduced adsorption under alkaline conditions (pH > 9), where red spheres represent Mg^{2+}/Fe^{3+} metal centers, while blue spheres denote hydroxyl groups or hydroxide ions involved in surface interactions and pH-dependent competition.

Adsorption kinetics

The adsorption kinetics of amoxicillin on MgFe-LDH and MgFe-CLDH were analyzed using the pseudo-first-order, pseudo-second-order, and Eelovich models. The corresponding kinetic models applied in this study include the pseudo-first-order, pseudo-second-order, and Elovich equations, as expressed in Eqs. (2) - (4), respectively [39-41].

$$q_t = q_e(1 - e^{-k_1 t}) \quad (2)$$

$$q_t = \frac{k_2 q_e^2 t}{1 + k_2 q_e t} \quad (3)$$

$$q_t = \frac{1}{\beta}\ln(1 + \alpha\beta t) \quad (4)$$

In these equations, q_t (mg/g) represents the amount of amoxicillin adsorbed at time t, while q_e (mg/g) is the equilibrium adsorption capacity. The constant k (min^{-1}) denotes the pseudo-order reaction rate constant ($g \cdot mg^{-1} \cdot min^{-1}$). In the Elovich model, α ($mg \cdot g^{-1} \cdot min^{-1}$) is the initial adsorption rate, and β ($g \cdot mg^{-1}$) is the desorption constant related to surface coverage and activation energy. The fitting graphs are shown in **Figure 7**.

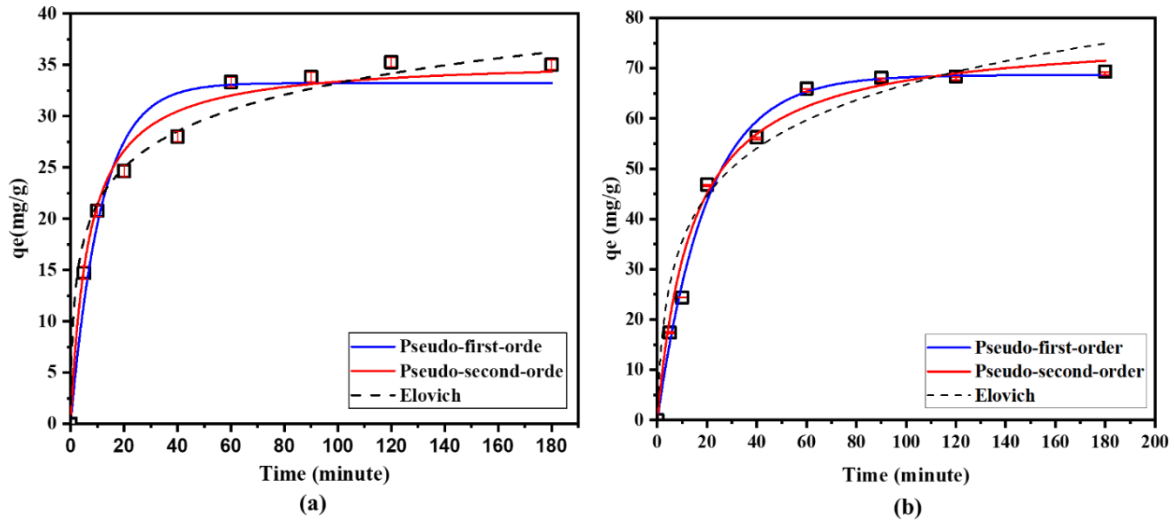

Figure 7 Amoxicillin adsorption kinetics on (a) MgFe-LDH and (b) MgFe-CLDH.

Figure 7(a) shows that the adsorption capacity of MgFe-LDH increased rapidly during the first 60 min, indicating strong initial interaction between the adsorbent surface and amoxicillin molecules. After this point, the adsorption rate gradually decreased as active sites became increasingly saturated, establishing 60 min as the optimal contact time. The kinetic parameters derived from model fitting are presented in

Table *2*. Among the evaluated models, the pseudo-second-order model exhibited the highest coefficient of determination (R^2 = 0.9901), indicating that the adsorption process is primarily governed by chemisorption involving surface interactions [40].

Table 2 Kinetic model parameters for MgFe-LDH.

Kinetic Model	Parameter	MgFe-LDH	MgFe-CLDH
Pseudo-first-order	$K_1(\mathrm{min}^{-1})$	0.0880	0.0504
	q_e (mg/g)	33.2328	68.6677
	R^2	0.9546	0.9928
Pseudo-second-order	$K_2(\mathrm{g \cdot mg^{-1} \cdot min^{-1}})$	0.0042	0.0009
	q_e (mg/g)	35.6160	77.1098
	R^2	0.9901	0.9759
Elovich	α $(\mathrm{mg \cdot g^{-1} \cdot min^{-1}})$	32.7843	16.3654
	β $(\mathrm{g \cdot mg^{-1}})$	0.1943	0.0714
	R^2	0.9350	0.9712

Similarly, MgFe-CLDH displayed a similar rapid uptake during the initial 60 min, as shown in **Figure 7(b)**, followed by a gradual approach toward equilibrium. The corresponding kinetic analysis also summarized in

Table *2* demonstrates that the pseudo-first-order model provided the best agreement with the experimental data (R^2 = 0.9928), suggesting that the adsorption rate is governed by the availability of unoccupied active sites on the surface of MgFe-CLDH. This behavior aligns well with the fundamental assumptions of the pseudo-first-order model and reflects the distinctive adsorption characteristics of the calcined derivative [41].

These kinetic differences between MgFe-LDH and MgFe-CLDH can be attributed to their distinct structural and surface chemical characteristics. MgFe-LDH retains a well-ordered layered structure with abundant –OH groups, which facilitates stronger surface

complexation and chemisorption with amoxicillin, consistent with its pseudo-second-order behavior [40]. In contrast, calcination converts MgFe-LDH into mixed metal oxides (MgFe-CLDH), reducing hydroxyl density, increasing surface heterogeneity, and promoting faster physisorption-dominated interactions. These properties align with the pseudo-first-order kinetics observed for MgFe-CLDH. Such trends are consistent with previous reports on LDH materials exhibiting memory-effect-induced structural changes after calcination [16].

Adsorption isotherm

Adsorption isotherm analysis was conducted to elucidate the interaction mechanism between amoxicillin and the adsorbents MgFe-LDH and MgFe-CLDH. The Langmuir isotherm assumes monolayer adsorption on a homogeneous surface with uniform adsorption sites, whereas the Freundlich isotherm accounts for multilayer adsorption on a heterogeneous surface with non-uniform energy distribution [42]. The isotherm Langmuir and Freundlich models are represented by Eqs. (5) and (6), respectively [43,44].

$$q_e = \frac{q_{max} K_L C_e}{1 + K_L C_e} \quad (5)$$

$$q_e = K_F C_e^{1/n} \quad (6)$$

where q_e is the equilibrium adsorption capacity (mg/g), C_e is the equilibrium concentration of amoxicillin (mg/L), q_{max} is the maximum adsorption capacity (mg/g), and K_L (L/mg) is the Langmuir constant related to the free energy of adsorption. In the Freundlich model, K_F is the Freundlich constant indicating adsorption capacity, and $1/n$ is a dimensionless parameter that reflects the adsorption intensity. A value of $0 < \frac{1}{n} < 1$ suggests favorable adsorption behavior. The fitting curves of the Langmuir and Freundlich models for both MgFe-LDH and MgFe-CLDH are illustrated in **Figure 8**.

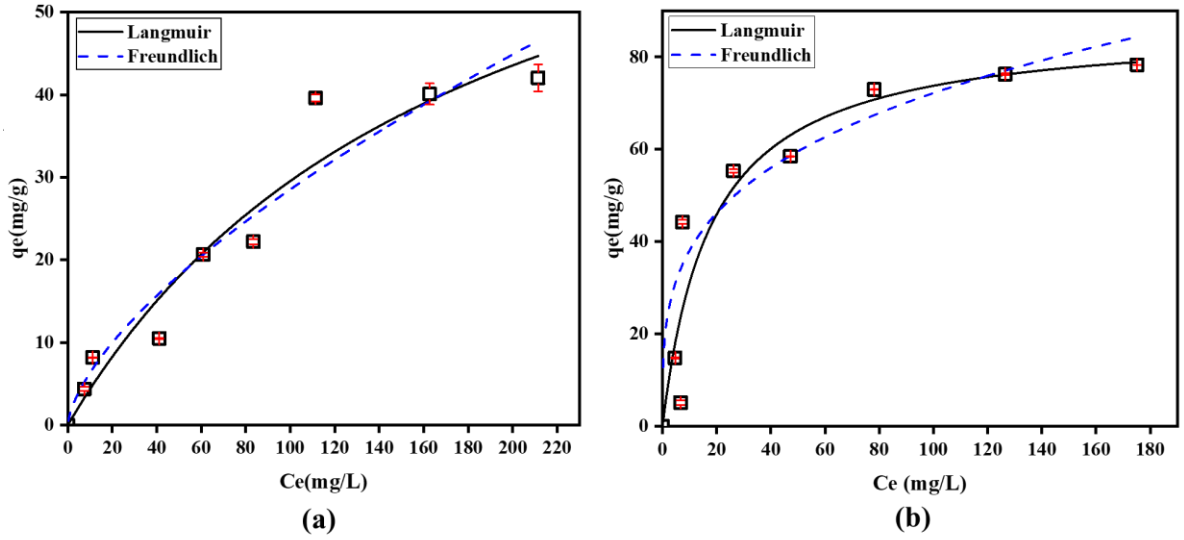

Figure 8 Adsorption Isotherm Graph of MgFe-LDH (a) and MgFe-CLDH (b).

The adsorption isotherm results show that both MgFe-LDH and MgFe-CLDH fit the Freundlich model better than the Langmuir model. As presented in **Figure 8(a)**, the adsorption of amoxicillin on MgFe-LDH follows the Freundlich model with a very high correlation (R^2 = 0.994), which is higher than that of the Langmuir model (R^2 = 0.934). A similar trend can be seen for MgFe-CLDH in **Figure 8(b)**, where the Freundlich model (R^2 = 0.928) also provides a better fit than the Langmuir model (R^2 = 0.902). The complete isotherm parameters for both adsorbents are summarized in **Table 3**, supporting the conclusion that the Freundlich model is more suitable.

Table 3 Isotherm model parameters for MgFe-LDH.

Isotherm Model	Parameter	MgFe-LDH	MgFe-CLDH
Langmuir	q_{max} (mg/g)	82.7949	86.9425
	K_L (L/mg)	0.0055	0.0559
	R^2	0.9342	0.9024
Freundlich	K_F (mg/g · (L/mg)$^{1/n}$)	0.6532	20.1415
	n	1.4092	0.2772
	R^2	0.9938	0.9281

As shown in **Table 3**, the better fit of the Freundlich model indicates that the adsorption of amoxicillin occurs on a heterogeneous surface and tends to form multilayer adsorption rather than a single uniform layer. This interpretation is consistent with the BET results, which show type III isotherm behavior (C < 1), suggesting relatively weak interactions between the adsorbent and amoxicillin but stronger interactions between amoxicillin molecules. These findings confirm that both MgFe-LDH and MgFe-CLDH possess surface properties conducive to multilayer adsorption phenomena. Additionally, the Freundlich model constant *n*, representing adsorption intensity constant, exceeding 1 for MgFe LDH (1.4) signifies substantial adsorption affinity in MgFe-LDH and MgFe-CLDH (0.2772) indicates more heterogeneous surfaces or stronger intensity.

Co-existing ion test

Various ions commonly present in water may interfere with the adsorption of amoxicillin. To assess this, selected representative ions were introduced into the system, and their effects on adsorption performance are illustrated in **Figure 9**.

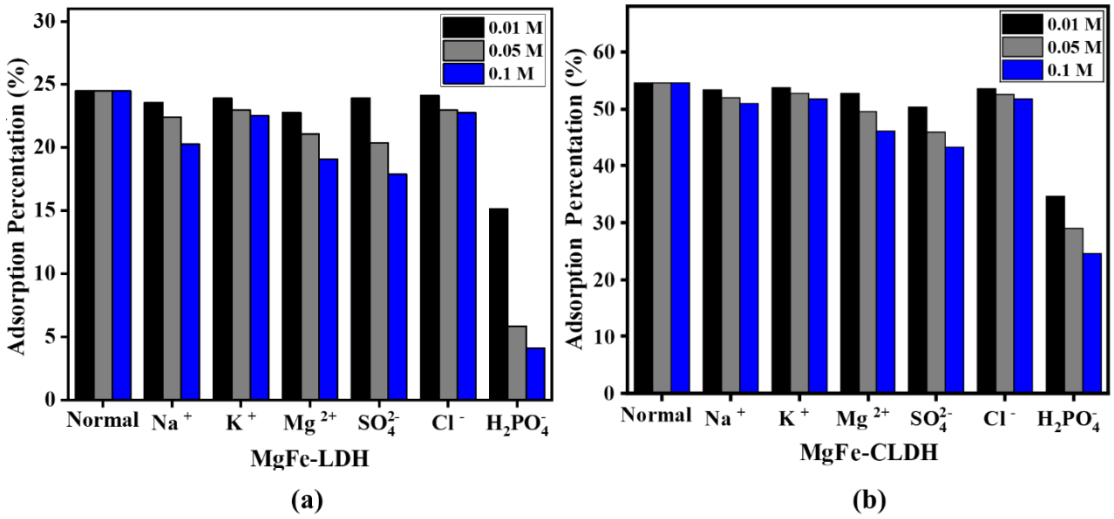

Figure 9 Effects of Co-Existing Ions on Amoxicillin Adsorption by (a) MgFe-LDH and (b) MgFe-CLDH.

The results indicate that the 3 tested cations (Na^+,K^+ and Mg^{2+}) did not significantly affect the adsorption of amoxicillin. This can be attributed to the LDH structure, which is more selective toward anion exchange, and the positively charged LDH surface, resulting from the presence of Mg and Fe, which reduces electrostatic interaction with cations. Among the anions tested, Cl^- also exhibited minimal interference with adsorption efficiency. This is likely due to its small ionic radius and weak interaction with the LDH surface compared to amoxicillin, which exhibits stronger adsorption through hydrogen bonding and π–π interactions, thereby outcompeting Cl^- for active sites. In contrast, SO_4^{2-} and $H_2PO_4^-$ anions significantly reduced the adsorption capacity. This effect is likely due to competitive adsorption, as these multivalent anions possess higher charge densities and stronger affinities for the LDH and CLDH surfaces. Additionally, their

molecular sizes and structures may enhance their ability to occupy adsorption sites, thereby limiting the availability of those sites for amoxicillin.

The effect of co-existing anions provides important insight into the adsorption mechanism of amoxicillin on MgFe-LDH and MgFe-CLDH. The pronounced reduction in adsorption capacity in the presence of multivalent anions (SO_4^{2-} and $H_2PO_4^-$) indicates strong competition for positively charged surface sites and suggests the involvement of electrostatic interactions and hydrogen bonding in the adsorption process. Although LDH intrinsically possess anion-exchange capability, XRD patterns (**Figure 3**) after adsorption show no significant shift in basal spacing, indicating that extensive intercalation of amoxicillin into the interlayer galleries is limited. Therefore, adsorption is dominated by surface complexation rather than interlayer anion exchange. Multivalent anions with higher charge density preferentially occupy surface hydroxyl groups, thereby suppressing amoxicillin uptake, which is consistent with FTIR results showing characteristic functional group vibrations of amoxicillin after adsorption. Similar adsorption behavior dominated by surface interactions rather than intercalation has been reported for amphoteric antibiotics on LDH-based adsorbents [43,45,46].

Structural analysis after adsorption

The SEM image, XRD, and FTIR analyses were used to investigate the structural variation of the adsorbent before and after adsorption. These characterization techniques complement each other in elucidating the morphological, crystallographic, and chemical interaction changes that occur upon amoxicillin adsorption.

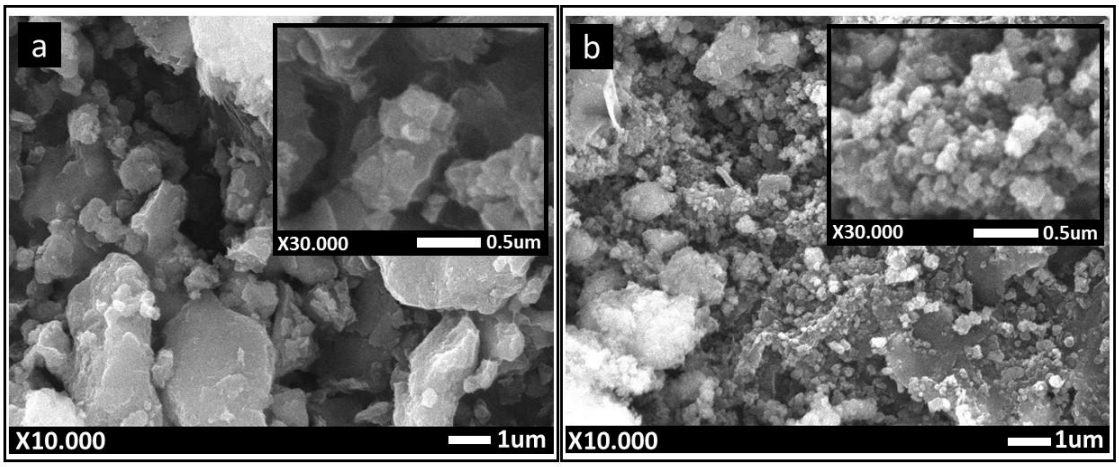

Figure 10 The SEM morphology of MgFe-LDH (a) and MgFe-CLDH (b) after adsorption.

As shown in **Figure 10**, the SEM analysis reveals clear morphological differences between MgFe-LDH and MgFe-CLDH after adsorption. **Figure 10(a)** shows the LDH structure after adsorption maintained its disc-like form, indicating that amoxicillin adsorption did not significantly alter the LDH morphology [43]. However, **Figure 10(b)** shows a more irregular and fragmented morphology. This behavior is likely associated with residual oxide phases that were not fully rehydrated after calcination. These remaining oxide regions, together with possible interactions with contaminants or amoxicillin molecules during adsorption, may contribute to the formation of small aggregated fragments observed in the micrographs [47,48]. These morphological observations are consistent with the XRD results presented in **Figure 3**. The XRD patterns of MgFe-LDH after adsorption (MgFe-LDH-AMX) and MgFe-CLDH after adsorption (MgFe-CLDH-AMX) exhibit the same peaks as those observed in MgFe-LDH, indicating that most of amoxicillin did not intercalate into the LDH structure. For MgFe-CLDH-AMX, the similarity of its diffraction peaks to those of MgFe-LDH further indicates a rehydration process that restores the LDH structure, confirming the well-known memory effect of calcined LDH materials [49]. A closer inspection reveals changes in peak intensities, particularly at around $2\theta \approx 61.5°$, indicating the partial participation of this plane in the adsorption process.

Further confirmation of amoxicillin adsorption is provided by FTIR spectra in **Figure 4**. After adsorption, new peaks were observed at approximately 2,960 and 1,250 cm^{-1}. The 2,960 cm^{-1} peak corresponds to the stretching vibrations of the CH_2 group on amoxicillin, and the 1,250 cm^{-1} peak represents the C–N and N–H bond vibrations of the secondary amide, indicating that amoxicillin has been absorbed on both adsorbents [50].

These findings support a plausible adsorption mechanism involving multiple interaction pathways. This adsorption mechanisms involved in MgFe-LDH and MgFe-CLDH systems include LDH interlayer anion exchange, electrostatic interactions, and hydrogen bonding between the adsorbent and the adsorbate [45]. While anion exchange is a commonly reported mechanism in LDH-type materials, it was not dominant in this study. This is supported by XRD analysis (**Figure 3**), which revealed no significant that amoxicillin did not intercalate into the interlayer region. The primary interaction responsible for adsorption is likely electrostatic attraction between the positively charged Mg and Fe ions and the negatively charged functional groups of amoxicillin. Due to the presence of 3 ionizable functional groups, amoxicillin exhibits pH-dependent speciation, with 3 pKa values, as shown in **Figure 11** [43].

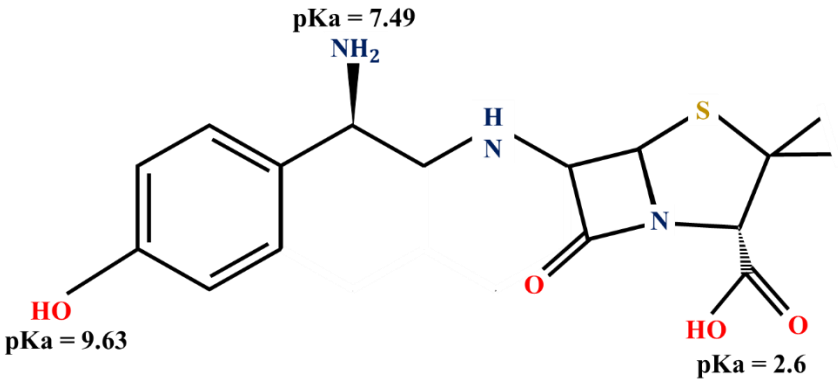

Figure 11 Amoxicillin functional groups and pka values.

At pH 4 and 6, amoxicillin exists predominantly in zwitterionic and anionic forms, where the amine group carries a positive charge and the carboxyl group carries a negative charge [51]. This allows for favorable electrostatic interactions with the adsorbent surface. Additionally, hydrogen bonding is also presumed to contribute to the adsorption process. At pH 4 and 6, the hydroxyl groups in amoxicillin are uncharged, enabling hydrogen bond formation with hydroxyl groups on the surface of both MgFe-LDH and MgFe-CLDH. Therefore, the adsorption of amoxicillin is likely governed by a synergistic mechanism involving electrostatic interactions and hydrogen bonding.

Regeneration study of MgFe-LDH

The regeneration or reuse of the nanoadsorbent is one of the significant economic factors in the water treatment process. This factor assists in understanding free from residual contaminants prior to reuse [43]. the mechanism of the pollutant adsorbed on the surface of the adsorbents as well reusing the spent adsorbents to save money and the environment from secondary pollution. The regeneration study was carried out on the MgFe-LDH sample only to see the memory effect of the adsorbent. Regeneration of MgFe-LDH was carried out via thermal calcination at 450 °C, a temperature reported to be optimal for the formation of active sites without inducing spinel phase transformation [52]. This method was selected due to the inherent memory effect of LDH materials, which enables the reconstruction of their layered structure upon rehydration post-calcination. Moreover, amoxicillin is known to undergo complete thermal degradation above 298 °C, meaning that calcination effectively removes the adsorbed antibiotic from the surface and ensures that the regenerated MgFe-LDH is

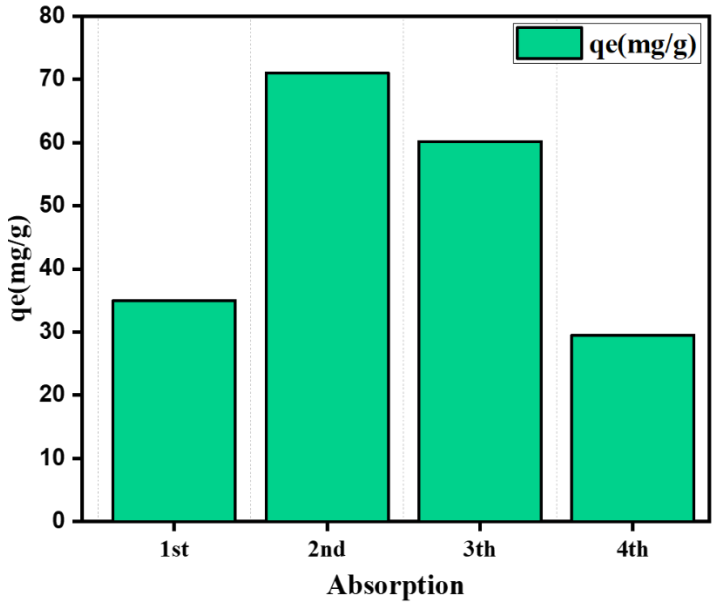

Figure 12 Regeneration of MgFe-LDH for amoxicillin adsorption.

As illustrated in **Figure 12**, the adsorption capacity increased from 35.02 mg/g in the first cycle to 71.01 mg/g in the second cycle. This increase is attributable to the memory effect of MgFe-LDH, where calcination transforms the material into mixed metal oxides (MgFe-CLDH) and subsequent rehydration during the second adsorption cycle reconstructs the layered LDH structure. Evidence of this structural recovery is supported by the XRD pattern of MgFe-CLDH after adsorption (**Figure 3**), which shows the reappearance of characteristic LDH reflections resembling pristine MgFe-LDH. Such reconstruction behavior has been widely reported for calcined LDH systems, where rehydration regenerates the layered architecture and exposes newly accessible hydroxyl sites, thereby enhancing adsorption performance [25,46].

However, adsorption performance declined in the following cycles, with capacities decreasing to 60.14 and 29.47 mg/g in the third and fourth cycles, respectively. This reduction is likely related to incomplete structural reconstruction, progressive pore blockage, and accumulation of residual adsorbates, which reduce available active sites. Overall, these results indicate that MgFe-LDH possesses regeneration capability through the memory effect, though adsorption efficiency tends to diminish after the second cycle.

Comparison of solid adsorbents, MgFe-LDH and MgFe-CLDH

The maximum adsorption capacity of silica nanoparticles for amoxicillin adsorption was compared with that of the other investigated adsorbents as demonstrated in **Table S2**. The data in **Table S2** illustrate that maximum adsorption capacity of MgFe-LDH and MgFe-CLDH are comparable to other solid adsorbents for amoxicillin removal from the polluted water.

Conclusions

In summary, MgFe-LDH and MgFe-CLDH adsorbents were successfully synthesized via the co-precipitation method and demonstrated effective performance for the removal of amoxicillin across a wide pH range. Kinetic modeling revealed that MgFe-LDH followed a pseudo-second-order kinetic model, while MgFe-CLDH fit the pseudo-first-order model, indicating distinct adsorption behaviors. The adsorption isotherms were better described by the Freundlich model, with maximum adsorption capacities reaching 82.79 mg/g for MgFe-LDH and 86.94 mg/g for MgFe-CLDH. Structural characterization before and after adsorption suggested that the mechanism likely involves chemisorption through electrostatic interactions and hydrogen bonding. Regeneration studies performed on

MgFe-LDH demonstrated an optimal adsorption capacity of 71.578 mg/g during the second adsorption cycle, followed by a gradual decline in subsequent cycles. These findings suggest that MgFe-based LDH materials are promising, environmentally friendly adsorbents for antibiotic removal in aqueous environments. The novelty of this study lies in the utilization of bittern, an abundant industrial by-product of salt production, as a sustainable and low-cost magnesium precursor for the synthesis of MgFe-LDH and MgFe-CLDH. In contrast to conventional MgFe-LDHs synthesized using analytical-grade magnesium salts (e.g., $Mg(NO_3)_2$ or $MgCl_2$), the bittern-derived materials demonstrate comparable adsorption capacities for amoxicillin, indicating that the substitution of commercial precursors does not compromise adsorption performance. Importantly, the use of bittern offers distinct advantages in terms of raw-material cost reduction, resource efficiency, and environmental sustainability. Moreover, the proposed synthesis route eliminates the need for additional purification or salt-preparation steps, underscoring the feasibility of valorizing industrial waste streams into functional adsorbents for wastewater treatment applications.

Acknowledgements

The authors are grateful to L'orèal For Women in Science National Fellowship, Research Organization of Nanotechnology and Materials and Research Organization of Life Science and Environment for the research funding. Also, for the Research Center for Environmental and Clean Technology - BRIN. The authors acknowledge the facilities, scientific and technical support from Advanced Characterization Laboratories Bandung, National Research and Innovation Agency E- Layanan Sains.

Declaration of generative AI in scientific writing

Only limited support from ChatGPT was utilized to rephrase certain sentences, while all scientific content, analysis, and conclusions were independently developed by the authors.

CRediT author statement

Swasmi Purwajanti: Conceptualisation, Methodology; Validation; Formal Analysis, Supervision, Funding acquisition and Writing-review draft preparation. **Jasmine Cupid Amaratirta:** Formal Analysis, Validation, Writing-original and editing. **Razita: Izzati**: Investigation and Formal Analysis. **Akmal Zulfi:** Validation, Formal Analysis and Writing-review and editing. **Yulianto Agung Rezeki:** Formal analysis**,** Funding acquisition and Writing - Review & Editing. **Nur Rohmah:** Validation and Formal Analysis. **Aep Patah:** Validation and Supervision

References

[1] SK Ahmed, S Hussein, K Qurbani, RH Ibrahim, A Fareeq, KA Mahmood and MG Mohamed. Antimicrobial resistance: Impacts, challenges, and future prospects. *Journal of Medicine, Surgery, and Public Health* 2024; **2**, 100081.

[2] MP Ferraz. Antimicrobial resistance: the impact from and on society according to one health approach. *Societies* 2024; **14(9)**, 187.

[3] A Huttner, J Bielicki, MN Clements, N Frimodt-Møller, AE Muller, JP Paccaud and JW Mouton. Oral amoxicillin and amoxicillin-clavulanic acid: properties, indications and usage. *Clinical Microbiology and Infection* 2020; **26(7)**, 871-879.

[4] Ö Kerkez-Kuyumcu, ŞS Bayazit and MA Salam. Antibiotic amoxicillin removal from aqueous solution using magnetically modified graphene nanoplatelets. *Journal of Industrial and Engineering Chemistry* 2016; **36**, 198-205.

[5] L Domínguez, M Eduard and D La Cruz. Working toward an environmental risk assessment of emerging contaminants in wastewater: The case of amoxicillin. *Water, Air, & Soil Pollution* 2025; **236**, 366.

[6] M Daliri, S Martinez-Morcillo, M Sharifinia, G Javdan and M Keshavarzifard. Occurrence and ecological risk assessment of antibiotic residues in urban wastewater discharged into the coastal environment of the Persian Gulf (the case of Bandar Abbas). *Environmental Monitoring and Assessment* 2022; **194(12)**, 905.

[7] C Li, A Li, X Hui, A Wang, LU Wang and S Chang. Concentrations, probabilistic human and ecological risks assessment attribute to antibiotics residues in river water in China: Systematic review and meta-analysis. *Ecotoxicology and Environmental Safety* 2024; **285**, 117022.

[8] KK Sodhi, M Kumar and DK Singh. Insight into

the amoxicillin resistance, ecotoxicity, and remediation strategies. *Journal of Water Process Engineering* 2021; **39**, 101858.

[9] S Li, Y Wu, H Zheng, H Li, Y Zheng, J Nan, J Ma, D Nagarajan and JS Chang. Antibiotics degradation by advanced oxidation process (AOPs): recent advances in ecotoxicity and antibiotic-resistance genes induction of degradation products. *Chemosphere* 2023; **311**, 136977.

[10] MW Nugraha, S Kim, F Roddick, Z Xie and L Fan. A review of the recent advancements in adsorption technology for removing antibiotics from hospital wastewater. *Journal of Water Process Engineering* 2025; **70**, 106960.

[11] P Pourhakkak, A Taghizadeh, M Taghizadeh, M Ghaedi and S Haghdoust. Fundamentals of adsorption technology. *Interface Science and Technology* 2021; **33**, 1-70.

[12] S Daniel and S Thomas. *Layered double hydroxides: Fundamentals to applications. In*: S Thomas and S Daniel (Eds.). Layered double hydroxide polymer nanocomposites. Woodhead Publishing, Cambridge, 2020.

[13] CO Okoye, R Nyaruaba, RE Ita, SU Okon, CI Addey, CC Ebido, AO Opabunmi, ES Okeke and KI Chukwudozie. Antibiotic resistance in the aquatic environment: analytical techniques and interactive impact of emerging contaminants. *Environmental Toxicology and Pharmacology* 2022; **96**, 103995.

[14] LF Ren, S Zhang, Z Ma, Y Qiu, D Ying, J Jia and Y He. Antibiotics separation from saline wastewater by nanofiltration membrane based on tannic acid-ferric ions coordination complexes. *Desalination* 2022; **541**, 116034.

[15] V Homem and L Santos. Degradation and removal methods of antibiotics from aqueous matrices - a review. *Journal of Environmental Management* 2011; **92(10)**, 2304-2347.

[16] AL Johnston, E Lester, O Williams and RL Gomes. Understanding layered double hydroxide properties as sorbent materials for removing organic pollutants from environmental waters. *Journal of Environmental Chemical Engineering* 2021; **9(4)**, 105197.

[17] DP De Lima, MF da Silva, AF da Silva, AH Ide and L Meili. Antibiotic removal from water using MgFe/layered double hydroxide as adsorbent. *In*: Proceedings of the 13th Brazilian Meeting on Adsorption EBA, Fortaleza, Brazil. 2020.

[18] Z Yang, C Zhang, G Zeng, X Tan, H Wang, D Huang, K Yang, J Wei, C Ma and K Nie. Design and engineering of layered double hydroxide based catalysts for water depollution by advanced oxidation processes: a review. *Journal of Materials Chemistry A* 2020; **8**, 4141-4173.

[19] C Park, J Song, G Lee and HJ Hong. Mechanistic study of direct Mg-Al layered double hydroxide formation for the removal of amphoteric ciprofloxacin (CIP) antibiotics from aqueous media. *Separation and Purification Technology* 2026; **367**, 132901.

[20] Z Yan, B Zhu, J Yu and Z Xu. Effect of calcination on adsorption performance of Mg-Al layered double hydroxide prepared by a water-in-oil microemulsion method. *RSC Advances* 2016; **6(55)**, 50128-50137.

[21] B Sulistiyo. *Analisis indikator kinerja utama kelautan dan perikanan Indonesia: Pengembangan perikanan budidaya* (*in Indonesian*). Pusat Data, Statistik, dan Informasi, Jakarta, Indonesia, 2017.

[22] A Tewari, HV Joshi, C Raghunathan, RH Trivedi and PK Ghosh. The effect of sea brine and bittern on survival and growth of mangrove *Avicennia marina* (Dicotyledones: Avicenniaceae). *Indian Journal of Marine Sciences* 2003; **32(1)**, 52-56.

[23] N Hafid, MB Belaatar, S Ben-Aazza, A Hadfi, M Ezahri and A Driouiche. Characterization of scale formed in drinking water and hot water pipes in the taliouine downtown-morocco. *American Journal of Analytical Chemistry* 2015; **6(8)**, 677.

[24] B Zeng, Q Wang, L Mo, F Jin, J Zhu and M Tang. Synthesis of Mg-Al LDH and its calcined form with natural materials for efficient Cr(VI) removal. *Journal of Environmental Chemical Engineering* 2022; **10(6)**, 108605.

[25] A Golban, L Lupa, L Cocheci and R Pode. Synthesis of MgFe layered double hydroxide from iron-containing acidic residual solution and its adsorption performance. *Crystals* 2019; **9(10)**, 514.

[26] YO Zubair, S Fuchida, K Oyama and C Tokoro.

Morphologically controlled synthesis of MgFe-LDH using MgO and succinic acid for enhanced arsenic adsorption: Kinetics, equilibrium, and mechanism studies. *Journal of Environmental Sciences* 2025; **148**, 637-649.

[27] Y Zhang, L Wang, L Zou and D Xue. Crystallization behaviors of hexagonal nanoplatelet $MgAlCO_3$ layered double hydroxide. *Journal of Crystal Growth* 2010; **312**, 3367-3372

[28] J Li, C Li, Q Tang, Z Zuo, L Liu and J Dong. Effect of MgFe-LDH with reduction pretreatment on the catalytic performance in syngas to light olefins. *Catalysts* 2023; **13(3)**, 632.

[29] DC Fletcher, R Hunter, W Xia, GJ Smales, BR Pauw, E Blackburn, A Kulak, H Xin and Z Schnepp. Scalable synthesis of dispersible iron carbide (Fe_3C) nanoparticles by 'nanocasting'. *Journal of Materials Chemistry A* 2019; **7(33)**, 19506-19512.

[30] J Kang, TG Levitskaia, S Park, J Kim, T Varga and W Um. Nanostructured MgFe and CoCr layered double hydroxides for removal and sequestration of iodine anions. *Chemical Engineering Journal* 2020; **380**, 122408.

[31] NBH Abdelkader, A Bentouami, Z Derriche, N Bettahar and LC De Menorval. Synthesis and characterization of Mg-Fe layer double hydroxides and its application on adsorption of orange G from aqueous solution. *Chemical Engineering Journal* 2011; **169(1-3)**, 231-238.

[32] BK Kim, GH Gwak, T Okada and JM Oh. Effect of particle size and local disorder on specific surface area of layered double hydroxides upon calcination-reconstruction. *Journal of Solid State Chemistry* 2018; **263**, 60-64.

[33] BH Alshammari, KD Alanazi, OA Sheej Ahmad, S Sallam, AH Al-Bagawi, AH Alsehli, BM Alshammari and NM El-Metwaly. Tailoring magnetic Sn-MOFs for efficient amoxicillin antibiotic removal through process optimization. *RSC Advances* 2024; **14(9)**, 5875-5892.

[34] MN Alnajrani and OA Alsager. Removal of antibiotics from water by polymer of intrinsic microporosity: Isotherms, kinetics, thermodynamics, and adsorption mechanism. *Scientific Reports* 2020; **10(1)**, 794.

[35] MF Abed and AA Faisal. Green synthesis of calcium/iron-layered double hydroxides-sodium alginate nanoadsorbent as reactive barrier for antibiotic amoxicillin removal from groundwater. *Adsorption Science & Technology* 2023. https://doi.org/10.1155/2023/1475278

[36] E Li, L Liao, G Lv, Z Li, C Yang and Y Lu. The interactions between three typical PPCPs and LDH. *Frontiers in Chemistry* 2018; **6**, 16.

[37] H Yuh-Shan. Citation review of Lagergren kinetic rate equation on adsorption reactions. *Scientometrics* 2004; **59(1)**, 171-177.

[38] HK Boparai, M Joseph and DM O'Carroll. Kinetics and thermodynamics of cadmium ion removal by adsorption onto nano zerovalent iron particles. *Journal of Hazardous Materials* 2011; **186(1)**, 458-465.

[39] YS Ho and G McKay. Pseudo-second order model for sorption processes. *Process Biochemistry* 1999; **34(5)**, 451-465.

[40] JC Bullen, S Saleesongsom, K Gallagher and DJ Weiss. A revised pseudo-second-order kinetic model for adsorption, sensitive to changes in adsorbate and adsorbent concentrations. *Langmuir* 2021; **37(10)**, 3189-3201.

[41] M Pająk, A Dzieniszewska and J Kyzioł-Komosińska. Natural (clinoptilolite) and synthetic (NaP1) zeolites in the adsorption process for the removal of acid black 1 dye from aqueous solutions. *Molecules* 2025; **30(8)**, 1677.

[42] BO Isiuku, PC Okonkwo and CD Emeagwara. Batch adsorption isotherm models applied in single and multicomponent adsorption systems - a review. *Journal of Dispersion Science and Technology* 2021; **42(12)**, 1879-1897.

[43] A Elhaci, F Labed, A Khenifi, Z Bouberka, M Kameche and K Benabbou. MgAl-layered double hydroxide for amoxicillin removal from aqueous media. *International Journal of Environmental Analytical Chemistry* 2021; **101(15)**, 2876-2898.

[44] KY Foo and BH Hameed. Insights into the modeling of adsorption isotherm systems. *Chemical Engineering Journal* 2010; **156(1)**, 2-10.

[45] Z Tang, Z Qiu, S Lu and X Shi. Functionalized layered double hydroxide applied to heavy metal ions absorption: A review. *Nanotechnology Reviews* 2020; **9(1)**, 800-819.

[46] YH Ye, S Liu, D Yu, X Zhou, L Qin, C Lai, F Qin, M Zhang, W Chen, W Chen and L Xiang. Regeneration mechanism, modification strategy, and environment application of layered double hydroxides: Insights based on memory effect. *Coordination Chemistry Reviews* 2022; **450**, 214253.

[47] K Takehira. Recent development of layered double hydroxide-derived catalysts - rehydration, reconstitution, and supporting, aiming at commercial application. *Applied Clay Science* 2017; **136**, 112-141.

[48] A Navajas, I Campo, A Moral, J Echave, O Sanz, M Montes, JA Odriozola, G Arzamendi and LM Gandía. Outstanding performance of rehydrated Mg-Al hydrotalcites as heterogeneous methanolysis catalysts for the synthesis of biodiesel. *Fuel* 2018; **211**, 173-181.

[49] W Xu, M Mertens, T Kenis, E Derveaux, P Adriaensens and V Meynen. Can high temperature calcined Mg-Al layered double hydroxides (LDHs) fully rehydrate at room temperature in vapor or liquid condition? *Materials Chemistry and Physics* 2023; **295**, 127113.

[50] T Bajda, A Grela, J Pamuła, J Kuc, A Klimek, J Matusik, W Franus, SKK Alagarsamy, T Danek and P Gara. Using zeolite materials to remove pharmaceuticals from water. *Materials* 2024; **17(15)**, 3848.

[51] D Hu and L Wang. Adsorption of amoxicillin onto quaternized cellulose from flax noil: Kinetic, equilibrium and thermodynamic study. *Journal of the Taiwan Institute of Chemical Engineers* 2016; **64**, 227-234.

[52] P Pinthong, P Praserthdam and B Jongsomjit. Effect of calcination temperature on Mg-Al layered double hydroxides (LDH) as promising catalysts in oxidative dehydrogenation of ethanol to acetaldehyde. *Journal of Oleo Science* 2019; **68(1)**, 95-102.

[53] P Pandey, A Shankar, M Biney and VK Saini. Enhancement in amoxicillin adsorption and regeneration properties of SBA-15 after surface modification with polyaniline. *Colloids and Interface Science Communications* 2021; **43**, 100432.

[54] JYJ Yeo, DS Khaerudini, FE Soetaredjo, GL Waworuntu, S Ismadji, J Sunarso and S Liu. Isotherm data for adsorption of amoxicillin, ampicillin, and doripenem onto bentonite. *Data in Brief* 2023; **48**, 109159.

[55] L El Azzouzi, S El Aggadi, M Ennouhi, A Ennouari, OK Kabbaj and A Zrineh. Removal of the Amoxicillin antibiotic from aqueous matrices by means of an adsorption process using Kaolinite clay. *Scientific African* 2022; **18**, e01390.

[56] L Ren, D Zhou, J Wang, T Zhang, Y Peng and G Chen. Biomaterial-based flower-like MnO_2@ carbon microspheres for rapid adsorption of amoxicillin from wastewater. *Journal of Molecular Liquids* 2020; **309**, 113074.

Supplementary Materials

Table S4 Structural parameters and statistical data of MgFe-LDH samples.

Field	Ref (°)	Experiment (°)	Relatif Error (%)
(003)	11.47	11.46	0.0871
(006)	23.36	23.35	0.0428
(009)	34.85	34.88	0.0860
(110)	60	59.51	0.8167
(113)	62	61.5	0.8064

Table S2 Comparison of AMX adsorption capacity of recent developed adsorbent.

Adsorbents	Qmax (mg/g)	References
SBA-15	24.7	[53]
PANI-SBA-15	34.2	[53]
BC	86.1	[54]
Kaoline clay	26.0	[55]
Flower-like MnO_2@ carbon microspheres	16.1	[56]
MgFe-LDH	82.79	This Study
MgFe-CLDH	86.94	This Study

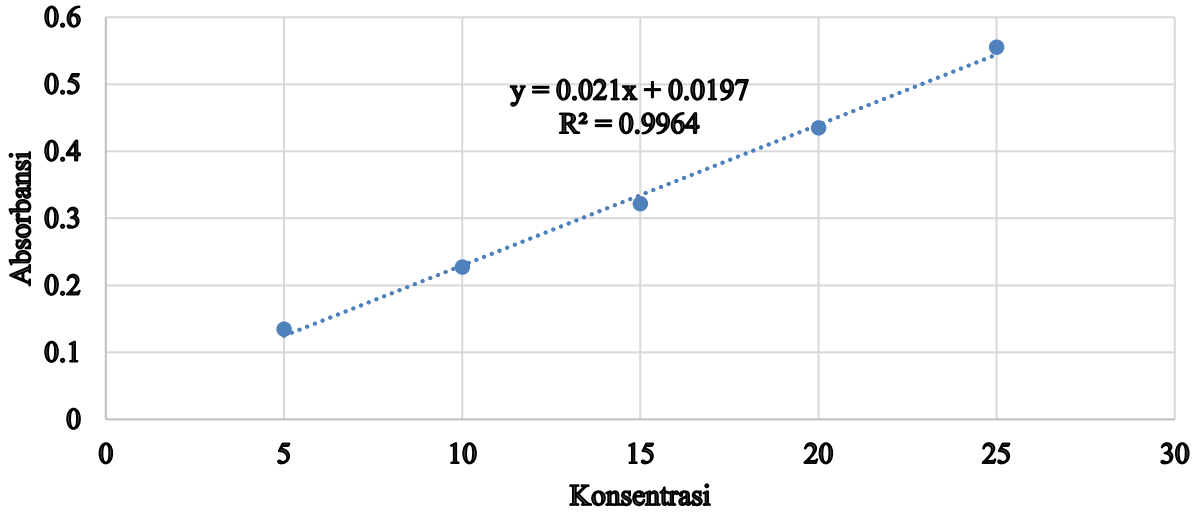

Figure S1 Calibration curve for amoxicillin quantification.